Control Strategy and Experiment of a Novel Hydraulic-Driven Upper Extremity Exoskeleton

Zirong Luo(✉), Guohen Wu, Xing Li, and Jianzhong Shang

National University of Defense Technology, Changsha 410073, Hunan, China
luozirong@nudt.edu.cn, l5lll460906@163.com

Abstract. In this paper, we introduce a novel hydraulic-driven upper extremity exoskeleton and present new type of force feedback control strategy, and the control experiment is also carried out. The experimental results show that the first generation upper extremity exoskeleton successfully follows the wearer's hand movements and achieve load capacity of 20 kg. The experimental results also indicate that the new type force feedback control can effectively reduce the interaction force between the wearer and the upper extremity exoskeleton and the oscillation. Compared with the control method simply using interaction force as the control input, the method with speed compensation controller can effectively reduce the amplitude and oscillation of the interaction force.

Keywords: Upper extremity exoskeleton · Hydraulic driven · Human-robot interaction technology · Force feedback control

1 Introduction

Exoskeleton technologies can bring new capabilities to fighting forces and improve endurance and safety in industrial settings [1, 2, 3]. The first functional load-carrying and energetically autonomous exoskeleton was demonstrated at U.C. Berkeley, walking at the average speed of 0.9 m/s (2 mph) while carrying a 34 kg (75 lb) payload. The original BLEEX sensitivity amplification controller, based on positive feedback, was designed to increase the closed loop system sensitivity to its wearer's forces and torques without any direct measurement from the wearer. And then Lihua Huang [4] from U.C. Berkeley presented an improved control scheme which added robustness to changing BLEEX backpack payload. Lockheed Martin [5] developed an unpowered, lightweight industrial exoskeleton called the FORTIS exoskeleton.

For the control of the exoskeleton, the wearer is directly responsible for most of the tasks in human computer interaction, such as command generation, environment perception, and motion feedback. The sensing and control system of exoskeleton needs to quickly perceive the wearer's intention to move, and to complete the precise following of the wearer's movements.

Kazerooni developed a 6-DOF upper extremity power-assist system which uses hydraulic pressure as the power source, through the interaction between a six component force sensor to measure the wear and the exoskeleton as control input [6].

Y. Huang et al. (Eds.): ICIRA 2017, Part I, LNAI 10462, pp. 51–62, 2017.
DOI: 10.1007/978-3-319-65289-4_5

Then, Caldwell developed a set of 7-DOF upper extremity exoskeleton, which also used the force sensors to measure the human-computer interaction force [7]. While Cavallaro estimated the torque needed by the upper extremity joints through EMG signal, and it was applied to a 7-DOF upper extremity exoskeleton [8]. However, the follow effect and the oscillation problems haven't been fully solved by the above achievements.

In this paper, a 3-DOF power-assist exoskeleton is studied, and the principle of realizing the exoskeleton control with the interaction force of the wearer and the exoskeleton is analyzed, and hence the direct force feedback control model of upper extremity exoskeleton is established. In the fast force feedback control model, the introduction of speed compensation is proposed to reduce the interaction force between the wearer and the exoskeleton, and the introduction of the compensation can greatly reduce the oscillation in the control. Finally, the effectiveness of the control model in the external force feedback control is verified by experiments.

2 The Control Strategy of the Upper Extremity Exoskeleton

2.1 The Role of Force in Control System

The wearer and the 3-DOF exoskeleton can be seen as one integrated control system composed of two sets of complete but interactive control systems, as shown in Fig. 1. Separately, the wearer controls his body movements through the brain, and the exoskeleton controls the rotation of the joint through the outer bone controller. Interactively, the wearer is regarded as the control input of the interaction system, and the controlled object is the upper extremity exoskeleton.

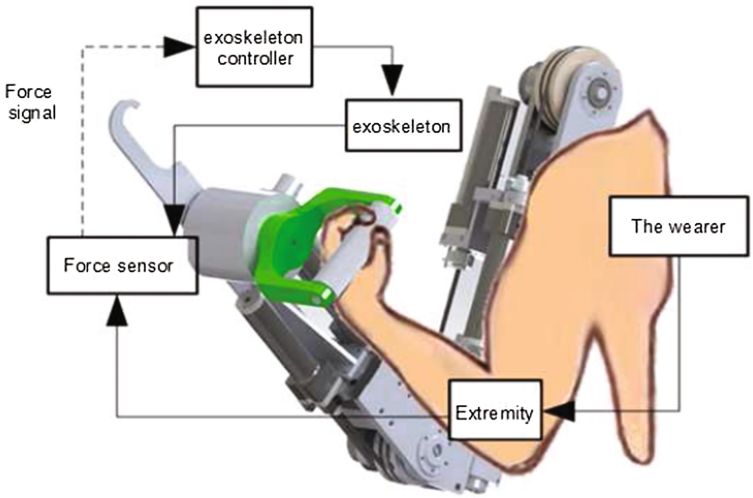

Fig. 1. The interactive interface of the exoskeleton

In this paper, we use one three dimensional force sensor to collect the interaction force between the wearer's hand and the handle of exoskeleton in order to analyze the intentions of wearers. As shown in Fig. 2(a), once the wearer gives his hand a force F, hands will begin to move relative with the exoskeleton's handle; but the exoskeleton has not realized the tracking in action yet, it still maintains the previous state, So the interaction force f is generated

$$F = f \tag{1}$$

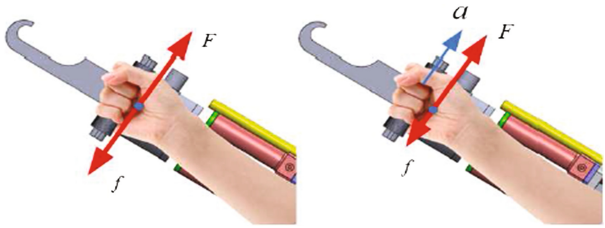

Fig. 2. The force of hands in x direction

At this moment, in order to reduce the force f the end of exoskeleton should move accelerately, as shown in Fig. 2(b). There is a balance equation among the force of the human hand, the force of the exoskeleton and the inertia force of the hand

$$f = F - M.a \tag{2}$$

In order to achieve the compliance following of the exoskeleton and the hands, the force f should be as small as possible. Under the constant force, through the Eq. (2), it is found that the effective way is to adjust the acceleration of the hands and the end of the exoskeleton. Also through Eq. (2), the force f reflects the size and direction of the acceleration, which can be used to predict the moving direction of the wearer's hand. The ideal value of f is 0. Equation (2) changes to $F = M.a$. Combining with the Eq. (1), we can get

$$a = Kf$$

Namely,

$$\begin{pmatrix} a_x \\ a_y \\ a_z \end{pmatrix} = \begin{pmatrix} k_x & 0 & 0 \\ 0 & k_y & 0 \\ 0 & 0 & k_z \end{pmatrix} \begin{pmatrix} f_x \\ f_y \\ f_z \end{pmatrix} \tag{3}$$

Where, K is the corresponding coefficient between the detected force and the acceleration, which is selected according to the debugging situation in real object.

2.2 The Relationship Matrix Between Force and Joint Angular Velocity

The spatial description of the end effector of the exoskeleton with respect to the fixed global coordinate system can be analyzed by D-H description method for kinematic analysis. A three degree of freedom upper extremity exoskeleton is shown in Fig. 3.

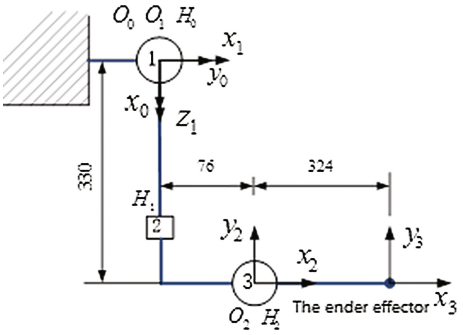

Fig. 3. The coordinate system of the link

In the coordinate system of the link, the transformation matrix can be described as

$$^{i-1}A_i = Rot(x_{i-1}, \alpha_{i-1})Trans(x_{i-1}, a_{i-1})Rot(z_i, \theta_i)Trans(z_i, d_i) \tag{4}$$

Where, a_i is the distance between z_{i-1} and z_i along x_i; x_i is the included angle between z_{i-1} and z_i around x_i; d_i is the distance between x_{i-1} and x_i along z_{i-1}; θ_i is the included angle between x_{i-1} and x_i around z_{i-1}. The transformation formula from the link to the moving coordinate is as follows

$$^0A_4 = {}^0A_1{}^1A_2{}^2A_3 \tag{5}$$

Through coordinate transformation, the relationship between the coordinates of the end effector of exoskeleton and the series of joint angle is established, and after the derivation of the both sides, we can get the Jacobian matrix of the upper extremity exoskeleton

$$\begin{aligned} X &= f(\theta), \\ \dot{X} &= J(\theta)\dot{\theta}, \end{aligned} \tag{6}$$

The inverse kinematics problem can be solved by Jacobi matrix inversion: $\dot{\theta}{=}J(\theta)^{-1}\dot{X}$

When there is an interaction force in x, y and z direction of the three dimensional force sensor, the corresponding displacement Δx, Δy, Δz are generated, and the corresponding joint angle change analysis is shown as Fig. 4(a)–(c)

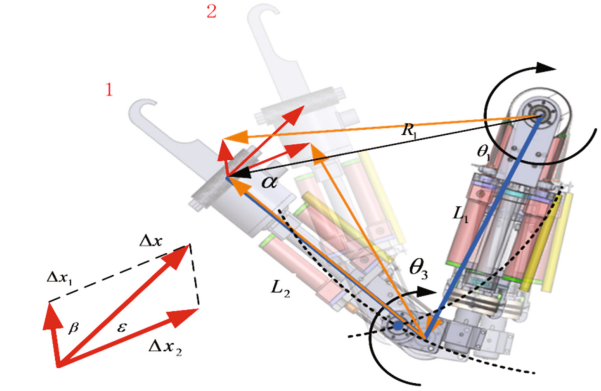

(a) Δx

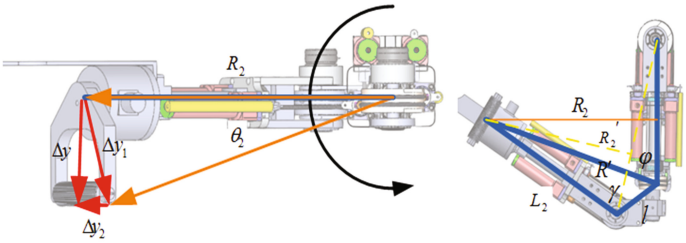

(b) Δy

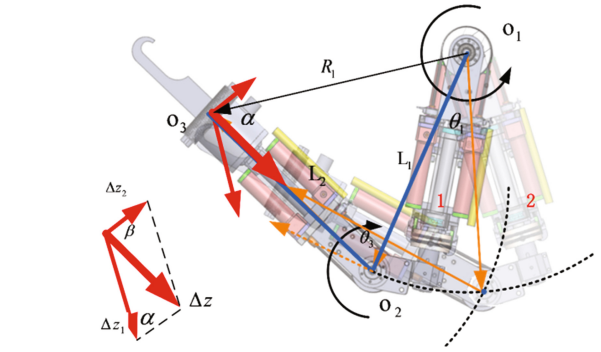

(c) Δz

Fig. 4. The corresponding change of angle

(1) As shown in Fig. 4(a), the corresponding displacement Δx can be calculated as

$$\Delta\vec{x} = \Delta\vec{x}_1 + \Delta\vec{x}_2 \tag{7}$$

In a control cycle, Δx is small enough, $\varepsilon \approx 0$, $\beta \approx 0$, $\Delta x_1 \approx 0$, $\Delta x_2 \approx 0$. Approximately, $\Delta x = \Delta x_2 = L_2 \bullet \Delta\theta_3$, and $\Delta\theta_3 = \Delta x / L_2$;

(2) As shown in Fig. 4(b), the corresponding displacement Δy can be calculated as

$$\Delta\vec{y} = \Delta\vec{y}_1 + \Delta\vec{y}_2 \tag{8}$$

In a control cycle, Δy is small enough, $\Delta y_1 = \sqrt{\Delta y^2 + \Delta y_2^2} \approx \Delta y$, $\Delta\theta_2 = \frac{\Delta y}{R_2}$, according to Cosine theorem, $R' = \sqrt{l^2 + L_2^2 - 2L_1L_2\cos\gamma}$, $R_2 = R'\sin\varphi = \sqrt{l^2 + L_2^2 - 2L_1L_2\cos\gamma} \times \sin\varphi$, and $\Delta\theta_2 = \frac{\Delta y_1}{R_2} \approx \frac{\Delta y}{\left(\sqrt{l^2 + L_2^2 - 2L_1L_2\cos\gamma} \times \sin\varphi\right)}$, when l is small, approximate processing can be carried out: $R_2 \approx R_2' = L_2 \times \sin\theta_3$, $\Delta\theta_2 = \frac{\Delta y_1}{R_2} \approx \frac{\Delta y}{R_2'} = \frac{\Delta y}{L_2 \times \sin\theta_3}$;

(3) As shown in Fig. 4(c), the corresponding displacement Δx can be calculated as

$$\Delta\vec{z} = \Delta\vec{z}_1 + \Delta\vec{z}_2 \tag{9}$$

In a control cycle, Δz is small enough, $\beta \approx 90°$, approximately $\Delta\overrightarrow{z_1} \perp \overrightarrow{o_1o_3}$, $\Delta\overrightarrow{z_2} \perp \overrightarrow{o_2o_3}$, $\Delta z_1 = R_1 \times \Delta\theta_1$, $\Delta z_2 = L_2 \times \Delta\theta_3$, according to Cosine theorem, $R_1 = \sqrt{L_1^2 + L_2^2 - 2L_1L_2\cos\theta_3}$, and according to Sine theorem, $\alpha = \angle o_1o_2o_3 = \arcsin\left(\frac{\sin\theta_3 \times L_1}{\sqrt{L_1^2 + L_2^2 - 2L_1L_2\cos\theta_3}}\right)$, and $\Delta z_1 = \frac{\Delta z}{\sin\alpha}$, $\Delta z_2 = \Delta z\cot\alpha$; So $\Delta\theta_1 = \frac{\Delta z_1}{R_1} = \frac{\Delta z}{L_1\sin\theta_3}$, $\Delta\theta_3 = \frac{\Delta z_2}{L_2} = \frac{\Delta z\cot\alpha}{L_2}$.

Based on above analysis in (1–3), the transform matrix T between moving velocity of the end of the handle and the rotation angular velocity of each joint is obtained. Suppose that the velocity of the end of the handle is $V = (\dot{x} \quad \dot{y} \quad \dot{z})$, the rotation angular velocity of each joint is $\omega = (\dot{\theta}_1 \quad \dot{\theta}_2 \quad \dot{\theta}_3)$, so $\omega = TV$, namely,

$$\begin{pmatrix} \dot{\theta}_1 \\ \dot{\theta}_2 \\ \dot{\theta}_3 \end{pmatrix} = \begin{pmatrix} 0 & 0 & \frac{1}{L_1\sin\theta_3} \\ 0 & \frac{1}{\sqrt{l^2 + L_2^2 - 2L_1L_2\cos\gamma} \times \sin\phi} & 0 \\ \frac{1}{L_2} & 0 & \frac{\cot\alpha}{L_2} \end{pmatrix} \begin{pmatrix} \dot{x} \\ \dot{y} \\ \dot{z} \end{pmatrix} \tag{10}$$

Where, $\alpha = \arcsin\left(\frac{\sin\theta_3 \times L_1}{\sqrt{L_1^2 + L_2^2 - 2L_1L_2\cos\theta_3}}\right)$.

After the derivation of $\omega = TV$, the geometrical transformation of acceleration can be obtained, the transform matrix T can be applied equally to detected components of acceleration in three directions.

2.3 The Control Strategy with Speed Compensation

The displacement data of the hydraulic cylinder is collected by the displacement sensor, and the linear relationship between the displacement of the hydraulic cylinder and the rotation angle of the joint is obtained by the geometric relation. It is

$$\begin{pmatrix} s_1 \\ s_2 \\ s_3 \end{pmatrix} = \begin{pmatrix} r_1 & 0 & 0 \\ 0 & r_2 & 0 \\ 0 & 0 & r_3 \end{pmatrix} \begin{pmatrix} \theta_1 \\ \theta_2 \\ \theta_3 \end{pmatrix}.$$

The on-off state of servo valve controls the movement direction and displacement of the hydraulic cylinder, the size of the valve opening size determines the speed of the hydraulic cylinder, the change rate of the opening size determines the acceleration of the hydraulic cylinder. The output of the servo valve is not only related to the angular acceleration $\dot{\omega}$ of the theoretical demand, but also the current angular velocity ω requires the servo valve to provide the corresponding flow rate. Speed compensation is introduced, so the control output of the servo valve is

$$E = f(\dot{\omega}) + f(\omega) \tag{11}$$

Where, $f(\dot{\omega})$ is the corresponding output of $\dot{\omega}$, $f(\omega)$ is the corresponding output of ω, combined with the above geometric relations, the relationship between output and speed signal and force signal can be obtained

$$E = f(\omega) + f(\dot{\omega}) = A_o R\omega + B_o R\dot{\omega} = A_o RTV + B_o R\dot{T}Kf \tag{12}$$

Where, $A_0 = \begin{pmatrix} a_1 & 0 & 0 \\ 0 & a_2 & 0 \\ 0 & 0 & a_3 \end{pmatrix}$, $B_0 = \begin{pmatrix} b_1 & 0 & 0 \\ 0 & b_2 & 0 \\ 0 & 0 & b_3 \end{pmatrix}$ are conversion factors related to hydraulic cylinder and hydraulic source, which can be determined according to the actual situation of the hydraulic system, such as hydraulic cylinder cross section, hydraulic pressure, the size of the valve port and etc.

The speed of the end of handle can be obtained by the integral of the acceleration, but the speed error will be accumulated with the increase of time due to the existence of system error. Therefore, speed compensation can be introduced by two methods:

(1) The angular velocity can be directly calculated through the displacement values collected by the displacement sensor, then, the current output value can be directly provided according to $E = A_0 R\omega + B_0 R\dot{T}Kf$;

(2) Assuming that the exoskeleton tracks well, the output value of the last control cycle can be used as the output value of the speed of last moment, namely, $E' = A_0 R\omega$, the current output is $E = E' + B_0 R\dot{T}Kf$, this method can be understood as a kind of incremental control method based on force signal.

3 Experiment and Discussion

In the experiment, the controlled object is shown in Fig. 5, which has 3 DOFs, and can be regarded as a serial mechanism.

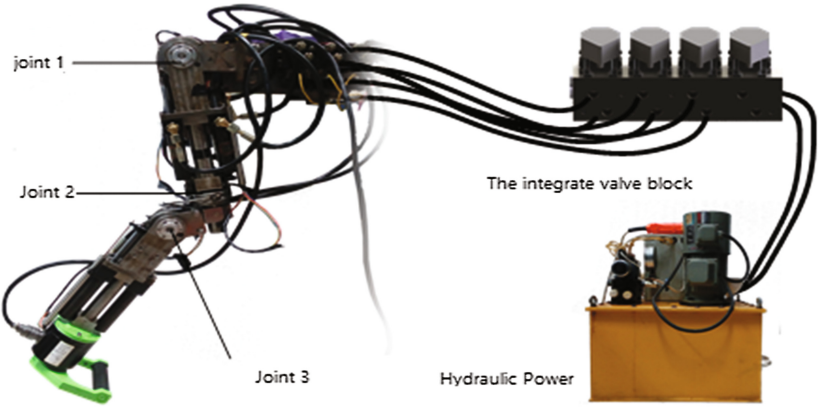

Fig. 5. The physical system

Figure 6 shows the control schematic of upper limb exoskeleton experiment system. The hardware system of the whole control loop is mainly composed of computer, sensors and data acquisition system.

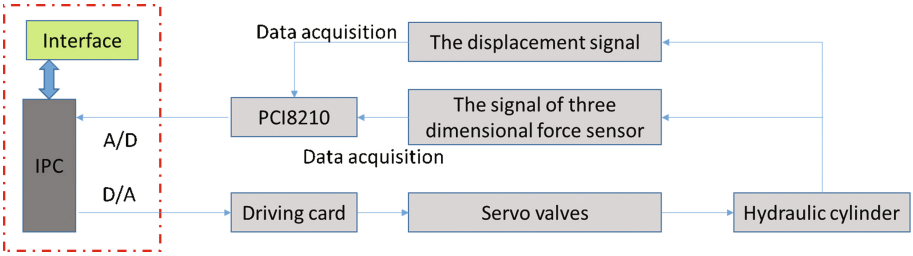

Fig. 6. The experiment system schematic of upper limb exoskeleton

According to Eq. (10),

$$T = \begin{pmatrix} 0 & 0 & \frac{1}{L_1 \sin\theta_3} \\ 0 & \frac{1}{\sqrt{l^2 + L_2^2 - 2L_1L_2\cos\gamma \times \sin\phi}} & 0 \\ \frac{1}{L_2} & 0 & \frac{\cot\alpha}{L_2} \end{pmatrix} \tag{1}$$

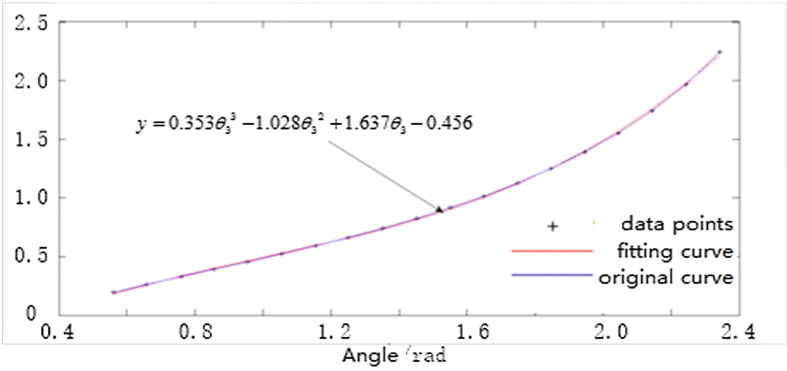

Fig. 7. The fitting results by cubic curves

Because $\frac{\cot\alpha}{L_2}$ is too complicated, in this example, it is fitted by cubic curves, as shown in Fig. 7.

So T is simplified as

$$T = \begin{pmatrix} 0 & 0 & \frac{1}{L_1 \sin\theta_3} \\ 0 & \frac{1}{L_2 \sin\theta_3} & 0 \\ \frac{1}{L_2} & 0 & \frac{\cot\alpha}{L_2} \end{pmatrix} = \frac{1}{L_2} \begin{pmatrix} 0 & 0 & \frac{0.96}{\sin\theta_3} \\ 0 & \frac{1}{\sin\theta_3} & 0 \\ 1 & 0 & 0.353\theta_3^3 - 1.028\theta_3^2 + 1.637\theta_3 - 0.456 \end{pmatrix} \quad (2)$$

Putting the simplified results into the control model, then, $E = A_0RTV + B_0R\dot{T}Kf$ can be obtained, and applying the control model to the experiment subjects. Adjust the parameters R, A_0, B_0, K to the best state. In fact, in the debugging process, not all the unknown parameters are debugged, which will lead the work to increase exponentially, and it's not necessary. Make $k_v = A_0RT$, $k_f = B_0R\dot{T}K$, and then set V and f as the inputs to debug the control model, thus, only two PID parameters are enough.

Fig. 8. The test path

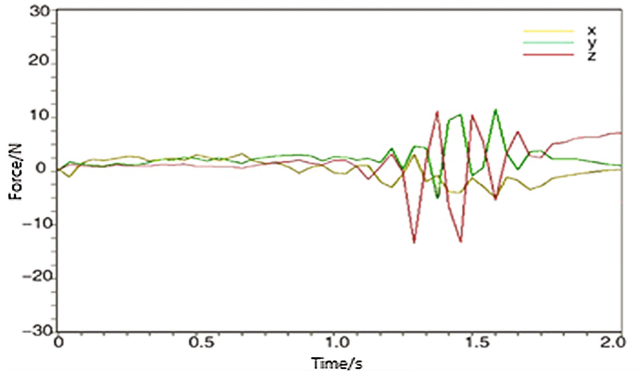

(a) Strategy without velocity compensation

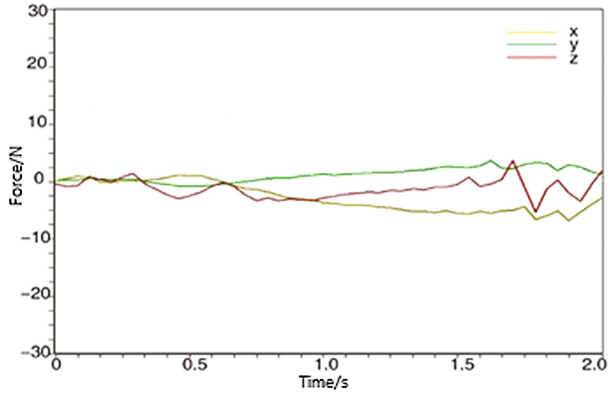

(b) Strategy I with velocity compensation

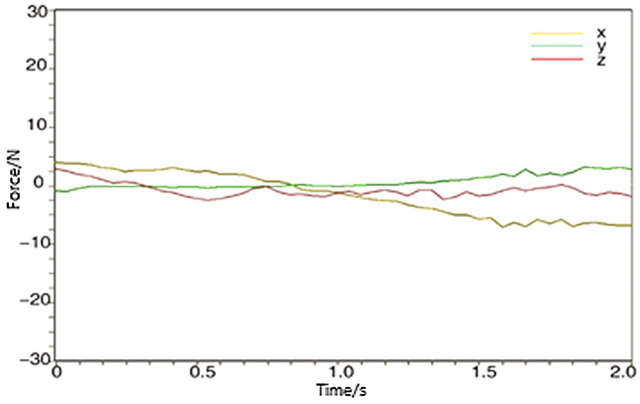

(c) Strategy II with velocity compensation

Fig. 9. The force curve of different control strategies

To validate the proposed control strategy in Sect. 2.3, the controlling tracking experiment is carried out to observe the influence of the angular velocity compensation on the control of exoskeleton; and the criterion is the magnitude of interaction force. In order to reduce the error of operation, each strategy is operated for 10 times.

As shown in Fig. 8, in the experiment, the operator pulls the end of the handle from point A to point B with a 20 kg object, then, the magnitude of the wearer's force can be detected.

Figure 9(a), (b) and (c) show the interaction force curves using different strategies, corresponding with strategy without velocity compensation, with velocity compensation by strategy I and by strategy II. We can see that:

(1) Compared with the simple force feedback control strategy (see Fig. 9(a)), the force feedback control strategy with the added speed compensation (see Fig. 9(b) and (c)) has not only less interaction force input, but also reduces the interaction force between the wearer and the exoskeleton. At the same time, with the addition of the velocity compensation, the oscillation is also obviously weakened, which shows that the direct force feedback control model with velocity compensation is more close to the real model of the upper extremity exoskeleton.

(2) In the two strategies with velocity compensation of direct force feedback control algorithm, the curve of strategy I (see Fig. 9(b)) is gentler than that of strategy II (see Fig. 9(c)). It may be caused by the deviation of the amount of compensation for the opening of the servo valve. Different from strategy I, strategy II is only concerned with the change of acceleration reflected by force.

4 Conclusion

In this paper, the exoskeleton control method focused on force signal with the introduction of angular velocity compensation is analyzed based on the interaction force between the wearer and the exoskeleton. The experimental results show that the hydraulic upper extremity exoskeleton can realize the wearer hand tracking and easily lift 20 kg weight. Compared with the control method simply using interaction force as the control input, the method with speed compensation controller can effectively reduce the amplitude and oscillation of the interaction force. It is suggested that in the future research, we can optimize the control hardware and reduce the micro oscillation.

References

1. Bergamasco, M., Frisoli, A., Avizzano, C.A.: Exoskeletons as man-machine interface systems for teleoperation and interaction in virtual environments. Springer Tracts Adv. Robot. **31**, 61–76 (2007)
2. Carignan, C.R., Naylor, M.P., Roderick, S.N.: Controlling shoulder impedance in a rehabilitation arm exoskeleton. In: IEEE International Conference on Robotics and Automation, IEEE explore, California, USA. pp. 2453–2458 (2008)

3. Romilly, D.P., Anglin, C., Gosine, R.G., Hershler, C., Raschke, S.U.: A functional task analysis and motion simulation for the development of a powered upper-limb orthosis. IEEE Trans. Rehabil. Eng. **2**(3), 119–129 (1994)
4. Kazerooni, H., Steger, R., Huang, L.: Hybrid control of the Berkeley lower extremity exoskeleton (BLEEX). Int. J. Robot. Res. **25**(25), 561–573 (2006)
5. Exoskeleton Technologies. http://www.lockheedmartin.com/us/products/exoskeleton.html. Accessed 03 Sept 2016
6. Kazerooni, H., Guo, J.: Human extenders. J. Dyn. Syst. Meas. Contr. **115**(2B), 281–290 (1993)
7. Caldwell, D., Tsagarakis, N., Kousidou, S., Costa, N., Sarakoglou, I.: Soft exoskeletons for upper and lower body rehabilitation–design, control and testing. Int. J. Humanoid Rob. **4**(3), 549–574 (2007)
8. Cavallaro, E., Rosen, J., Perry, J., Burns, S.: Real-time myoprocessors for a neural controlled powered exoskeleton arm. IEEE Trans. Biomed. Eng. **53**(11), 2387–2396 (2006)